Contents

1 Control of Spatially Extended Chaotic Systems

R. O. Grigoriev

1.1 Introduction

In the present chapter we consider a class of phenomena such as turbulence [1], plasma [2] and combustion [3] instabilities, cardiac arrhythmia [4], and brain epilepsy [5], which manifest themselves as an irregular chaotic behavior occurring in spatially extended nonlinear systems. Learning to control this irregular behavior is very attractive due to a large number of potential applications. Some practically important systems displaying spatiotemporal chaos are continuous, such as chemical reactors [6] or multi-mode lasers [7], some are discrete: neural networks [8] and power grids are only a few examples.

Unfortunately, most high-dimensional systems, those just mentioned included, remain notoriously difficult to control and little progress has been made so far in the implementation of existing control techniques [9, 10] due to a number of practical limitations. Although spatially extended homogeneous systems could be treated as a special case of high-dimensional chaotic systems [11, 12, 13], some of the practical issues that arise in the control problem are quite specific and are probably best handled by taking into account the spatiotemporal structure of the system and the controlled state in general, and their symmetry properties in particular [14].

In what follows we attempt to develop a general control algorithm for spatiotemporally chaotic systems using the linear-quadratic control (LQC) approach, which has become one of the cornerstones of modern control theory [15]. It is not accidental that we choose it over many variations [12, 13, 16] of the OGY control technique [17]. The idea and methodology of LQC is rooted in the theory of stochastic processes familiar to physicists and mathematicians alike. Besides, LQC alone provides a framework for the systematic and consistent treatment of both the steady and time-periodic control problem with or without noise, using full or partial information about the system state.

To make the general discussion more specific we select a model system which, on the one hand, has the dynamics and the spatiotemporal structure characteristic of extended spatiotemporally chaotic systems in general, and, on the other hand is simple enough to analyze and compute. Since spatially extended systems typically show rotational and translational symmetries, we require the model system to be symmetric as well. In order to facilitate the analysis we also require the model to be finite-dimensional, which puts the system on a spatial lattice. Furthermore, since the analysis of continuous- and discrete-time systems is very similar, we choose to discretize time as well. It can be argued that the results obtained after this reduction are still applicable to extended systems, continuous or discrete in space as well as time.

In general, the dynamics of the model system at time t depends deterministically on its present state, which we denote $\mathbf{x}^t$, and on the values of system parameters $\mathbf{u}$. However, the state of any finite-dimensional approximation cannot fully represent the state of the actual infinite-dimensional system. The evolution of the state $\mathbf{x}^t$ should, therefore, also depend on the unmodeled dynamics of unaccounted degrees of freedom, which might include unknown interaction with the environment. Consequently, the evolution equation should include both deterministic and stochastic components. The effect of the latter is usually rather small and can be treated as random noise $\mathbf{w}^t$, often called the process noise:

$$\mathbf{x}^{t+1} = \mathbf{F}(\mathbf{x}^t, \mathbf{w}^t, \mathbf{u}). \tag{1.1.1}$$

Since interactions in extended physical systems often have a rather short range, if we associate one degree of freedom x_i^t with each site i of the spatial lattice, we can neglect the dependence of the dynamics of a variable x_i^t on the variables x_j^t associated with all lattice sites j, except the few nearest neighbors of the site i. (We do not consider systems with long range interactions here to avoid unnecessarily complicating the discussion, although they can be treated equally successfully using the formalism outlined below.) For simplicity the lattice can be chosen as one-dimensional, and then our reduced model is naturally represented by a stochastic generalization of the deterministic coupled map lattice (CML) with nearest neighbor diffusive coupling [18]:

$$x_i^{t+1} = \epsilon f(x_{i-1}^t, a) + (1-2\epsilon) f(x_i^t, a) + \epsilon f(x_{i+1}^t, a) + L_i(\mathbf{x}^t, \mathbf{w}^t), \tag{1.1.2}$$

where index $i = 1, 2, \cdots, n_x$ labels the lattice sites, and the last term (we assume $L_i(\mathbf{x}, \mathbf{0}) = 0$ for every i and $\mathbf{x}$) represents the net effect of stochastic perturbations at site i. Imposing the periodic boundary condition, $x_{i+n_x}^t = x_i^t$, emulates the translational (or rotational for, e.g., a Taylor Couette system) invariance. We take $\mathbf{u} = (a, \epsilon)$, and assume that both a and ϵ are the same throughout the lattice.

The local map $f(x, a)$ can be chosen as an arbitrary (nonlinear) function with parameter a, which typically represents the process of generation of chaotic fluctuations by the local dynamics of the system, while diffusive coupling typically plays the opposite role of dissipating local fluctuations. Therefore, the parameters a and ϵ specify the degree of instability and the strength of dissipation in the system, respectively. For the purpose of control, however, details of the local map are not

important. The only aspect of the control problem affected by any particular choice is the set of existing unstable periodic trajectories.

Our ultimate goal is to construct a linear control scheme able to stabilize any steady or time-periodic state of the CML (1.1.2) of arbitrary length n_x in the presence of nonzero noise and assuming that complete information about the state of the system is unavailable and has to be extracted from the noisy time series measurement of a limited number of scalar observables. Furthermore, we would like the control scheme to provide optimal performance with or without noise and be practically realizable. The major ingredients of such a control scheme are expected to be system-independent and, hence, applicable to extended spatiotemporally chaotic systems in general.

The rest of the chapter is organized as follows. We start in section 1.2 with finding the appropriate control parameters. Section 1.3 is devoted to control of steady target states in the absence of noise. The results are generalized to noisy systems in section 1.4 and then to time-periodic target states in section 1.5. The modifications necessary when full information about the state of the system is unavailable are discussed in section 1.6. In section 1.7 we determine the number of independent control parameters necessary to control the noisy system of arbitrary length. Finally, section 1.8 summarizes the major results.

1.2 Control Parameters

1.2.1 Conditions for Control

Before we proceed with the analysis of the general problem of controlling arbitrary time-periodic target states of our noisy model (1.1.2) based on partial measurements of the state, we study the simplest case of linear steady state control in the absence of noise and assuming the full knowledge of the state of the system. The solution for the general case is then obtained as a sequence of rather straightforward generalizations. The first problem that we face here is that there is no natural choice of control parameters in the problem. Besides, as we will see shortly, not every control parameter is suitable.

In order to determine the restrictions imposed by the structure of the system on the control parameters we need to linearize the evolution equation (1.1.2) about the selected target state

$$\bar{\mathbf{x}} : \ \bar{\mathbf{x}} = \mathbf{F}(\bar{\mathbf{x}}, \mathbf{0}, \bar{\mathbf{u}}). \tag{1.2.1}$$

Denoting $\Delta\mathbf{x}^t = \mathbf{x}^t - \bar{\mathbf{x}}$ the deviation from the target trajectory (1.2.1) and $\Delta\mathbf{u}^t = \mathbf{u}^t - \bar{\mathbf{u}}$ the perturbation of the parameter vector, one obtains for small $\Delta\mathbf{x}^t$ and $\Delta\mathbf{u}^t$

$$\Delta\mathbf{x}^{t+1} = A\Delta\mathbf{x}^t + B\Delta\mathbf{u}^t, \tag{1.2.2}$$

where the matrix $A = D_{\mathbf{x}}\mathbf{F}(\bar{\mathbf{x}}, \mathbf{0}, \bar{\mathbf{u}})$ represents the Jacobian of the system and $B = D_{\mathbf{u}}\mathbf{F}(\bar{\mathbf{x}}, \mathbf{0}, \bar{\mathbf{u}})$ is the control matrix, reflecting the linear response to the variation of parameters, both evaluated at the target state $\bar{\mathbf{x}}$. Specifically, we have $A = MN$, where

$$M_{ij} = (1 - 2\epsilon)\delta_{i,j} + \epsilon(\delta_{i,j-1} + \delta_{i,j+1}) \tag{1.2.3}$$

is the constant coupling matrix (with $\delta_{i,j\pm1}$ extended to comply with periodic boundary condition), and

$$N_{ij} = \partial_x f(\bar{x}_i, a)\delta_{i,j} \tag{1.2.4}$$

is the state-dependent stretching matrix.

The dynamics of the CML (1.1.2) can be made stable in the vicinity of the target state $\bar{\mathbf{x}}$ by applying appropriate perturbations $\Delta\mathbf{u}^t$, if the matrices A and B satisfy the *stabilizability* condition [15], i.e., when there exists a linear synchronous feedback

$$\Delta\mathbf{u}^t = -K\Delta\mathbf{x}^t, \tag{1.2.5}$$

where K is the *feedback gain* matrix, such that all eigenvalues of the matrix $A' = A - BK$ are stable (have magnitude smaller than one, $|\lambda_k| < 1$, $\forall k$). Indeed, plugging feedback (1.2.5) into Eq. (1.2.2) one obtains the linearized evolution equation for the closed-loop system

$$\Delta\mathbf{x}^{t+1} = (A - BK)\Delta\mathbf{x}^t, \tag{1.2.6}$$

with $\Delta\mathbf{x} = \mathbf{0}$ becoming the stable fixed point of the map (1.2.6).

In practice, however, imposing the more stringent *controllability* condition on the matrices A and B often produces better results. The system (1.2.2), or the pair of matrices (A, B), is called controllable if, for any initial state $\Delta\mathbf{x}^{t_i} = \Delta\mathbf{x}_i$, times $t_f - t_i \geq n_x$, and final state $\Delta\mathbf{x}_f$, there exists a sequence of control perturbations $\Delta\mathbf{u}^{t_i}, \cdots, \Delta\mathbf{u}^{t_f-1}$ such that the solution of Eq. (1.2.2) satisfies $\Delta\mathbf{x}^{t_f} = \Delta\mathbf{x}_f$. The controllability condition is satisfied whenever

$$\operatorname{rank}[\,B \quad AB \quad \cdots \quad (A)^{n_x-1}B\,] = n_x \tag{1.2.7}$$

and automatically ensures stabilizability.

There is a number of reasons to choose the controllability condition over the stabilizability condition. The most important of those is the fact that the latter usually sensitively depends on the equilibrium values of system parameters (in our case a and ϵ), while the former does not. This is especially important if the same control setup is to be used for different values of parameters, or the target trajectory is to be tracked as the values of parameters slowly change. Besides, it is much easier to test a system for controllability using Eq. (1.2.7) than for stabilizability — the latter essentially requires finding the feedback (1.2.5) which might be a daunting problem in itself.

1.2.2 Symmetry, Locality and Pinning Control

Careful analysis of the controllability condition shows [14] that if the system is symmetric, certain symmetry-imposed restrictions on the choice of control parameters should be satisfied in order to achieve control. In fact, our model is by construction highly symmetric. The symmetry is that of the spatial lattice: the evolution equation (1.1.2) is invariant with respect to translations by an integer number of sites and with respect to reflections about any site (or midplane between any adjacent sites), which map the lattice back onto itself without destroying the adjacency

relationship. The respective symmetry group for the lattice with n_x sites and the periodic boundary condition is $\mathcal{G} = \mathrm{C}_{n_x v}$.

Without repeating the symmetry analysis conducted in [14], we mention two major results which are especially important for us. First of all, irrespectively of the length of the lattice n_x, it is impossible to control *every* target state of the CML (1.1.2) using a single control parameter. However, an arbitrary target state can be controlled using two (or more) independent control parameters. The minimal number of control parameters depends on the symmetry properties of the target state, and the higher the symmetry is, the stricter requirements are imposed on the control scheme. Since we are looking to construct a general control scheme independent of the details of each particular target state, we assume that at least two control parameters should be available.

Second, it is impossible to control symmetric target states using global system parameters, such as a and ϵ. As a consequence, feedback has to be applied *locally*. On the other hand, practical considerations would suggest that it is much easier to perturb the system locally at a number of distinct spatial locations, e.g., applying local fields, local pressure gradients, injecting chemical reactants, etc. This type of feedback represents interaction with the control plant considered to be a part of the environment, and cannot be adequately described using only the internal system parameters like those characterizing the rate of growth of local chaotic fluctuations and the strength of spatial dissipation. Instead, it is most naturally described by generalizing the term $L_i(\mathbf{x}^t, \mathbf{w}^t)$ in Eq. (1.1.2) to include the interaction with the control plant, so that

$$x_i^{t+1} = \epsilon f(x_{i-1}^t, a) + (1-2\epsilon) f(x_i^t, a) + \epsilon f(x_{i+1}^t, a) + L_i(\mathbf{x}^t, \mathbf{w}^t, \mathbf{u}^t), \qquad (1.2.8)$$

where now vector $\mathbf{u}^t$ describes the strength of interaction with the control plant. The equilibrium value $\bar{\mathbf{u}}$ can be selected arbitrarily, so we will assume $\bar{\mathbf{u}} = \mathbf{0}$ below. Without noise and control the last term in Eq. (1.2.8) vanishes, so one should have $\mathbf{L}(\mathbf{x}, \mathbf{0}, \mathbf{0}) = \mathbf{0}$. Consequently, the linearization about the target state $\bar{\mathbf{x}}$ again yields Eq. (1.2.2), but now with $B = \mathbf{D_u L}(\bar{\mathbf{x}}, \mathbf{0}, \mathbf{0})$.

For simplicity we further assume that the interaction between the system and the control plant is limited to only a few lattices sites i_m, which we call pinnings following Gang and Zhilin [9]:

$$\frac{\partial L_i(\mathbf{x}, \mathbf{w}, \mathbf{0})}{\partial u_j} = 0 \qquad (1.2.9)$$

for all $\mathbf{x}$, $\mathbf{w}$ and $i \neq i_m$, $m = 1, 2, \cdots, n_u$. Then, without loss of generality, the control matrix B can be chosen as a matrix with dimensions $n_x \times n_u$:

$$B_{ij} = \sum_{m=1}^{n_u} \delta_{j,m} \delta_{i,i_m}, \qquad (1.2.10)$$

such that Δu_m^t describes the strength of the control perturbation applied at the lattice site $i = i_m$. The number of pinnings (equal to the number of control parameters) can be, in principle, chosen arbitrarily in the range $\bar{n}_u \leq n_u \leq n_x$, where $\bar{n}_u = 2$ as we established above.

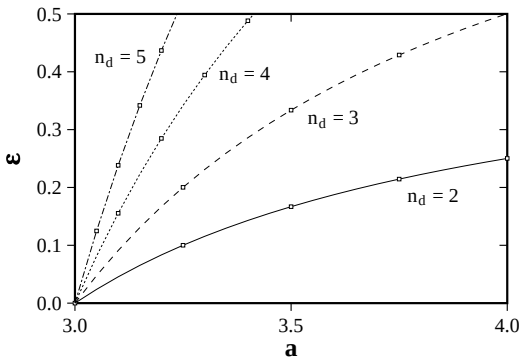

Abb. 1.1: Periodic array of single pinning sites: minimal coupling ϵ as a function of parameter a. The dots represent the numerical results from Fig. 2 of Ref. [9], with ϵ rescaled by a factor of two to make it compatible with our definition.

1.2.3 Periodic Array of pinnings

Symmetric target states are arguably the most practically interesting and important of all, so these will be the focus of the discussion that follows. It is no accident that by far the most common target state, a spatially uniform time-invariant state $\bar{x}_1 = \cdots = \bar{x}_{n_x} = \bar{x}$, is the state with the highest symmetry, and, as a consequence, the most difficult state to control as well. On the other hand, symmetry usually significantly simplifies the analysis of system dynamics, and the neighborhood of the uniform target state benefits most from this simplification. All of this makes it the perfect target state to test the general results on. Since the steady uniform state is period one in both space and time, we will often use the shorthand notation S1T1 for it.

Naively it seems that the most natural choice is to place the pinnings in a periodic array, such that the distance between all n_u pinnings is constant, $i_{m+1} - i_m = n_d$, $\forall m$. However, it can be shown [9] that with this setup the uniform target state could only be stabilized with a rather dense array of pinnings, and that the distance n_d sensitively depends on the values of system parameters a and ϵ. Figure 1.1 shows the minimal coupling ϵ for which the stabilization was achieved numerically as a function of a for several values of n_d for the logistic local map

$$f(x, a) = ax(1 - x) \tag{1.2.11}$$

with the fixed point $\bar{x} = 1 - a^{-1}$. In particular, in the physically interesting interval of parameters $3.57 < a < 4.0$ where the independent logistic maps are chaotic, control fails unless $n_d \leq 3$. It is interesting to note, that the distance between periodically placed pinnings can be increased significantly if the symmetry of the system is lower, such as when the parity symmetry is broken [19].

One can easily verify that the matrix (1.2.10) calculated for a periodic array of pinning sites does not satisfy the controllability condition. Since the uniform state is invariant with respect to both translations and reflections of the lattice,

the eigenfunctions of the Jacobian

$$A = \partial_x f(\bar{x}, a) M \tag{1.2.12}$$

coincide with eigenfunctions of the operators of translation and reflection, which are well known to be given by Fourier modes $\mathbf{g}^i$:

$$g^i_j = \cos(jk_i + \phi_i). \tag{1.2.13}$$

Here ϕ_i are arbitrary phase shifts, and k_i are the wavevectors defined thus: $k_1 = 0$, $k_i = k_{i+1} = \pi i/n_x$ for $i = 2, 4, 6, \cdots$, and, for n_x-even, $k_{n_x} = \pi$. Fourier modes with the same wavevectors k define invariant subspaces of the Jacobian, $L^k \subset R^{n_x}$.

Let us denote $\mathbf{b}_i$ the ith column of the matrix B. According to the analysis conducted in [14], the controllability condition is only satisfied when the projections of the vectors $\mathbf{b}_i$, $i = 1, \cdots, n_u$ span every invariant subspace L^k. The pinnings are placed with period n_d, so

$$(\mathbf{g}^i \cdot \mathbf{b}_m) = \cos((i_1 + (m-1)n_d)k_i + \phi_i) = 0 \tag{1.2.14}$$

for every m, whenever $\phi_i = i_1 k_i + \pi/2$ and $k_i = \pi/n_d, 2\pi/n_d, 3\pi/n_d, \cdots$. As a consequence, only a one-dimensional subspace of L^{k_i} will be spanned, while $\dim(L^k) = 2$, $0 < k < \pi$. In other words, feedback through the periodic array of pinnings does not affect the modes (1.2.13) whose nodes happen to lie at the pinnings, i.e. modes with periods $2\pi/k_i$ equal to $2n_d$, $2n_d/2$, $2n_d/3$, etc, provided those are integer. Such modes are called *uncontrollable*.

The control succeeds only when *all* uncontrollable modes are stable, i.e., when the weaker stabilizability condition is satisfied. This, however, imposes excessive restrictions on the density of pinnings $\rho = n_u/n_x$, again due to the spatial periodicity of the array. The condition for stabilizability can be obtained from the spectrum of eigenvalues of the Jacobian matrix (1.2.12):

$$\gamma_i = \alpha(1 - 2\epsilon(1 - \cos(k_i)), \tag{1.2.15}$$

where $\alpha = \partial_x f(\bar{x}, a) = 2 - a$. Specifically, we need

$$\left| (a-2) \left[1 - 2\epsilon \left(1 - \cos\left(\frac{\pi j}{n_d} \right) \right) \right] \right| < 1 \tag{1.2.16}$$

for all $j = 1, \cdots, n_x - 2$, such that n_d/j is integer. Using this criterion one can obtain the relation between the minimal coupling, the distance between pinnings n_d, and parameter a of the local chaotic map for a stabilizable system. For instance, $j = 1$ yields

$$\epsilon = \frac{a-3}{2(a-2)\left(1 - \cos\left(\frac{\pi}{n_d}\right)\right)}. \tag{1.2.17}$$

The curves defined by Eq. (1.2.17) are plotted in Fig. 1.1 together with the numerical results of Gang and Zhilin [9] and are seen to be in excellent agreement. Alternatively Eq. (1.2.17) can be used to find the maximal value of n_d as a function

of a and ϵ for the target state S1T1. Similar restrictions on the minimal density of pinnings can be obtained for target states of arbitrary spatial and temporal periodicity (e.g., S2T1 and S1T2 [20]).

As it was suggested in [21], one can get rid of all uncontrollable modes placing pinning sites differently. This will enable us to control the system *anywhere* in the parameter space at the same time using a *smaller* number of pinnings, simplifying the control setup. Let us take the minimal number, $n_u = 2$. In fact, two independent control parameters are enough to guarantee the controllability of *any* target state of the CML (1.2.8), irrespectively of the state's symmetry properties. In the absence of noise this translates into being able to control arbitrary steady or time periodic states of the coupled map lattice with an arbitrary (but finite) length, track target states as the system parameters change and so on, which ensures extreme flexibility of the control scheme.

The controllability condition for the matrices (1.2.12) and (1.2.10) imposes certain restrictions on the mutual arrangement of the pinnings i_1 and i_2: the length of the lattice n_x should not be a multiple of the distance between pinnings $|i_2 - i_1|$, otherwise the mode with the period $2|i_2 - i_1|$ becomes uncontrollable. One particular arrangement, however, is especially interesting: applying feedback through the pinnings placed at the "beginning" $i_1 = 1$ and the "end" $i_2 = n_x$ of the lattice is equivalent to controlling a spatially uniform system of finite length adjusting the boundary conditions.

1.3 Steady State Control

The next step in the algorithm is to determine the feedback $\Delta\mathbf{u}^t$ that would actually stabilize the target state $\bar{\mathbf{x}}$. At first we assume that complete information about the state of the system is available, i.e., the state vector $\mathbf{x}^t$ can be directly determined at any time step t. The feedback obtained using this assumption is usually called *state* feedback. Although a large assortment of linear state feedback control techniques is available (see, for example, review by Lindner and Ditto [22]), most of them are single-parameter. Those that employ multi-parameter control [9, 12, 16] are poorly suited to deal with stochastic dynamical systems and cannot be generalized to handle the *output* feedback control problem, which arises when complete information about the state of the controlled system is unavailable.

Instead we use linear-quadratic control theory [15], which, as we will see below, is perfectly suitable to deal with the above problems in a consistent manner. Another significant advantage of the proposed approach is the possibility to tune the feedback to obtain the best performance for a specific system. The performance of a control scheme is not a very well defined concept, so we will explicitly discuss what is implied in each particular case.

When the nonlinear dynamical system is completely deterministic, say

$$\mathbf{x}^{t+1} = \mathbf{F}(\mathbf{x}^t, \mathbf{u}), \tag{1.3.1}$$

any stabilizing linear feedback

$$\mathbf{u}^t = \bar{\mathbf{u}} - K[\mathbf{x}^t - \bar{\mathbf{x}}] \tag{1.3.2}$$

will eventually (and usually rather fast) bring the system arbitrarily close to the target state $\bar{\mathbf{x}}$, provided the system is in the neighborhood $\mathcal{N}(\bar{\mathbf{x}})$ of the target state when the control is turned on. The neighborhood $\mathcal{N}(\bar{\mathbf{x}})$ can be defined as the basin of attraction of the steady state $\bar{\mathbf{x}}$ of the nonlinear closed-loop system

$$\mathbf{x}^{t+1} = \mathbf{F}(\mathbf{x}^t, \bar{\mathbf{u}} - K[\mathbf{x}^t - \bar{\mathbf{x}}]). \tag{1.3.3}$$

The major difference between linear control algorithms is, therefore, in the size and shape of the basin of attraction.

We assume that the dynamics of the system is chaotic, i.e., the system evolves ergodically on a chaotic attractor $\mathcal{A}$ with a fractal structure, so that the system visits every neighborhood of any steady or periodic state embedded into the attractor as time goes on. Therefore, a natural (and often the only possible) way to enforce linear control for a target state $\bar{\mathbf{x}} \in \bar{\mathcal{A}}$ is to wait, with the control turned off, until the systems gets in the neighborhood $\mathcal{N}(\bar{\mathbf{x}})$ of the target state and then turn the control on. However, it is difficult to check if the condition $\mathbf{x} \in \mathcal{N}(\bar{\mathbf{x}})$ is satisfied, since the shape of the basin of attraction is usually very irregular.

In practice one instead checks for $\mathbf{x} \in \mathcal{P}(\bar{\mathbf{x}})$, where $\mathcal{P}(\bar{\mathbf{x}}) \subset \mathcal{N}(\bar{\mathbf{x}})$ is a regularly shaped neighborhood of $\bar{\mathbf{x}}$, which best approximates $\mathcal{N}(\bar{\mathbf{x}})$. The linear size δx of $\mathcal{P}(\bar{\mathbf{x}})$ is extremely important, especially for high-dimensional systems like the one we study here, because it determines the probability for the system to visit this neighborhood, which scales as $(\delta x)^{\mathcal{D}}$, where $\mathcal{D}$ is the local pointwise dimension of the attractor, and thus defines the average time t_c one has to wait to turn the control on (also called the *capture* time). Therefore, both the size and the shape of the neighborhood $\mathcal{N}(\bar{\mathbf{x}})$ are of ultimate importance if the linear control algorithm is to be practically effective.

The size of $\mathcal{N}(\bar{\mathbf{x}})$ crucially depends on the assumptions made during the derivation of the linear control law. In particular, the linear approximation (1.2.2) is valid only when both the deviation $\Delta\mathbf{x}^t$ from the target state and the perturbation $\Delta\mathbf{u}^t$ of the control parameters are sufficiently small, so that the combined state-plus-parameter vector belongs to a neighborhood $\mathcal{M}(\bar{\mathbf{x}}, \bar{\mathbf{u}}) \subset R^{n_x} \times R^{n_u}$ of the point $(\bar{\mathbf{x}}, \bar{\mathbf{u}})$ inside of which nonlinear corrections are negligible. Choosing the feedback gain K produces the constraint (1.3.2) projecting the set $\mathcal{M}(\bar{\mathbf{x}}, \bar{\mathbf{u}})$ onto the state space R^{n_x}, giving a first-order approximation

$$\mathcal{N}^{(1)}(\bar{\mathbf{x}}) = \{\forall \mathbf{x} \mid (\mathbf{x}, \bar{\mathbf{u}} - K[\mathbf{x} - \bar{\mathbf{x}}]) \in \mathcal{M}(\bar{\mathbf{x}}, \bar{\mathbf{u}})\}. \tag{1.3.4}$$

of the basin of attraction $\mathcal{N}(\bar{\mathbf{x}})$ (one has to ensure that Eq. (1.2.2) is valid for all consecutive steps as well, i.e., $\bar{\mathbf{x}} + (A - BK)^t(\mathbf{x} - \bar{\mathbf{x}}) \in \mathcal{N}^{(1)}(\bar{\mathbf{x}})$, $t = 1, 2, \cdots$). As a result, the feedback gain K usually has to be chosen such that the control perturbation $\Delta\mathbf{u}$ is minimized in order to maximize the size of $\mathcal{N}^{(1)}(\bar{\mathbf{x}})$. Such feedback can be found as an optimal solution, which minimizes the functional

$$V(\Delta\mathbf{x}^0) = \sum_{t=0}^{\infty} \left[H_s(\Delta\mathbf{x}^t) + H_c(\Delta\mathbf{u}^t)\right], \tag{1.3.5}$$

with the constraint (1.2.2) for every initial deviation $\Delta\mathbf{x}^0$. We introduced the following notations here:

$$H_s(\Delta\mathbf{x}) \quad = \quad \Delta\mathbf{x}^\dagger Q \Delta\mathbf{x},$$

$$H_c(\Delta\mathbf{u}) \quad = \quad \Delta\mathbf{u}^\dagger R \Delta\mathbf{u}, \tag{1.3.6}$$

where † denotes the matrix transpose, and Q and R are the feedback parameters, which could be chosen as arbitrary positive semidefinite symmetric matrices in order to tune the control scheme by "weighting" different components of the state and control vectors. However, since the system (1.2.8) is translationally invariant, it is often natural to choose the weight matrices as multiples of a unit matrix:

$$\begin{aligned} Q &= qI, \quad q \geq 0, \\ R &= rI, \quad r \geq 0, \end{aligned} \tag{1.3.7}$$

so that a single adjustable parameter, $q/r > 0$, remains instead of $n_x^2 + n_u^2$ matrix elements.

Although the dynamics of the system is in general non-Hamiltonian, it is interesting to note the following analogy with mechanical description of Hamiltonian systems: $H_s(\Delta\mathbf{x})$ and $H_c(\Delta\mathbf{u})$ can be interpreted as the Hamiltonian function of the linearized system and the energy of its interaction with the control plant, so that the functional $V(\Delta\mathbf{x})$ represents the discrete-time action.

Using variational calculus it can be trivially shown that the minimal value of the action (1.3.5) is reached for $\Delta\mathbf{u}^t = -K\Delta\mathbf{x}^t$ and is quadratic in the initial deviation, $V(\Delta\mathbf{x}) = \Delta\mathbf{x}^\dagger P \Delta\mathbf{x}$, where P is the solution of the discrete-time algebraic Riccati equation

$$P = Q + A^\dagger PA - A^\dagger PB(R + B^\dagger PB)^{-1} B^\dagger PA, \tag{1.3.8}$$

which essentially is the discrete-time version of the Hamilton-Jacobi equation, and the feedback gain K is given by:

$$K = (R + B^\dagger PB)^{-1} B^\dagger PA. \tag{1.3.9}$$

It can be shown [15] that, if R is positive definite, $Q = D^\dagger D$ and the pairs (A, B) and $(A^\dagger, D^\dagger)$ are controllable, there exists a unique positive definite solution P to Eq. (1.3.8), and the closed loop system (1.2.6) with feedback gain (1.3.9) is stable. Formally, the derivation of the Riccati equation is only valid for $R \neq 0$. However, since the limit

$$P = \lim_{R \to 0} P(R) \tag{1.3.10}$$

is usually well defined, the Riccati equation can be used to find the optimal feedback for $R = 0$ as well. Although it is generally impossible to find the solution of the Riccati equation analytically, extensive software exists for solving nonlinear matrix equations of this type numerically. The easiest way to find the solution P numerically is by direct iteration of Eq. (1.3.8).

Numerical simulations show that the CML defined by Eqs. (1.2.8) and (1.2.11) can be stabilized by the linear control (1.2.5) with feedback gain (1.3.9) in a wide range of parameters a and ϵ, as we expected. For $a = 4.0$ and $\epsilon = 0.33$ the steady uniform state of the lattice with length $n_x = 8$ has three unstable and five stable eigenmodes. We use two pinning sites, located at the "boundaries", $i_1 = 1$ and $i_2 = 8$, to control the system. This corresponds to

$$L_i(\mathbf{x}^t, \mathbf{w}^t, \mathbf{u}^t) = \delta_{i,1} u_1^t + \delta_{i,8} u_2^t. \tag{1.3.11}$$

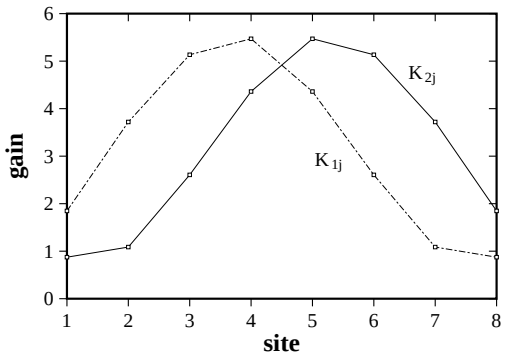

Abb. 1.2: Optimal feedback gain for the steady state S1T1: feedback gains K_{1j} and K_{2j} for the two pinnings placed at the sides of the lattice ($i_1 = 1, i_2 = 8$) as functions of the lattice site j for $a = 4.0$ and $\epsilon = 0.33$.

The solution for K is presented graphically in Fig. 1.2 for the choice $Q = I$, $R = I$. Naturally, the contribution $K_{mj}\Delta x_j^t$ from the site j far away from the pinning site i_m is larger: since the feedback is applied indirectly through coupling to the neighbors, the perturbation introduced at the pinnings decays with increasing distance from the pinning sites.

Fig. 1.3(a) shows the state of the system as the evolution takes it along a trajectory which passes through the neighborhood $\mathcal{N}(\bar{\mathbf{x}})$ of the uniform target state, and subsequently as control, turned on at time $t = 0$, drives the system towards the target state. One can see that even though the dimensionality of the system is much larger than the number of control parameters, it only takes about ten time steps for the observable deviations from the uniform configuration to disappear. One can obtain a more quantitative description of the convergence speed by looking at the standard deviation

$$\sigma_x^t = \left[\frac{1}{n_x} \sum_{i=1}^{n_x} |\Delta x_i^t|^2 \right]^{1/2} \tag{1.3.12}$$

from the uniform target state with $\bar{x} = 1 - a^{-1} = 0.75$ as a function of time, presented in Fig. 1.3(b) along with the magnitude of control perturbations Δu_1^t and Δu_2^t.

1.4 Control in the Presence of Noise

When the external noise is not negligible, $\mathbf{w}^t \neq \mathbf{0}$, the control problem has to be considerably reformulated. First of all, feedback still has to be chosen such that the closed-loop system is stable. However, the system will never converge exactly to the target state, since noise will continuously drive it away. Therefore, now the objective of control is to keep the system as close as possible to the target state for

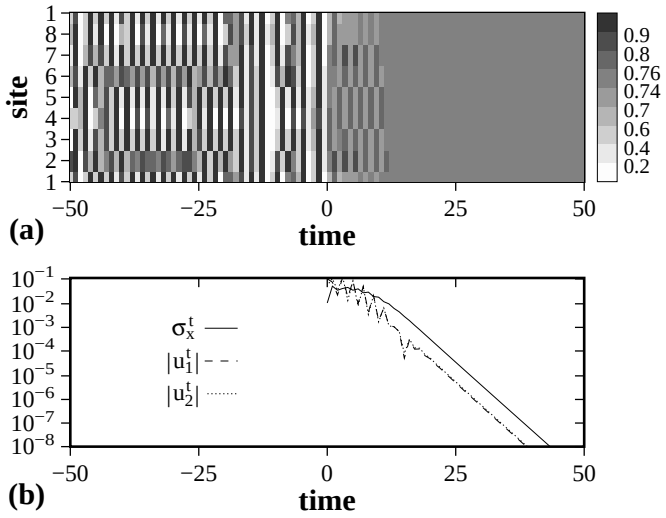

Abb. 1.3: State feedback control of the steady state S1T1: (a) system state, (b) its deviation σ_x^t from the target state and magnitude of control perturbations u_1^t and u_2^t. Feedback is turned on at $t = 0$.

arbitrary magnitude of noise. Second, the system becomes stochastic and has to be described probabilistically instead of deterministically. In particular, Eq. (1.2.2) is replaced with

$$\Delta\mathbf{x}^{t+1} = A\Delta\mathbf{x}^t + B\Delta\mathbf{u}^t + E\mathbf{w}^t, \tag{1.4.1}$$

where we defined $E = \mathbf{D_w L}(\bar{\mathbf{x}}, \mathbf{0}, \mathbf{0})$.

Similarly to the deterministic case, linearization (1.4.1) has to be valid in order for linear control to succeed. Consequently, the range of permissible deviations $\Delta\mathbf{x}^t$ from the target trajectory is again maximized by minimizing the control perturbation $\Delta\mathbf{u}^t$, which brings us back to the functional (1.3.5). A few changes should be made, however, in keeping with the probabilistic description of the problem. To make the value of the functional (1.3.5) independent of noise, we average it over all possible noise signals $\mathbf{w}^0, \mathbf{w}^1, \cdots$. In addition, we replace the infinite sum with the infinite time average to ensure convergence:

$$V = \left\langle \lim_{T\to\infty} \frac{1}{T} \sum_{t=0}^{T} \left[H_s(\Delta\mathbf{x}^t) + H_c(\Delta\mathbf{u}^t) \right] \mid \Delta\mathbf{x}^0 = \Delta\mathbf{x}_i \right\rangle . \tag{1.4.2}$$

Suppose, the noise is described by a stationary zero-mean random process $\mathbf{w}^t$, which is δ-correlated in time, such that[1]

$$\langle \mathbf{w}_t \mathbf{w}_{t'}^\dagger \rangle = \Xi\, \delta_{tt'}, \tag{1.4.3}$$

where Ξ is the correlation matrix of the process. Then the minimum of the functional (1.4.2) is again reached for $\Delta\mathbf{u}^t = -K\Delta\mathbf{x}^t$, but now it is quadratic in noise

[1] We choose to lower the time index where appropriate for notational convenience.

[15], $V = \mathrm{Tr}(PE\Xi E^\dagger)$, and is independent of the initial displacement $\Delta\mathbf{x}_i$. The matrix P is again calculated as the solution of the Riccati equation (1.3.8), and the feedback gain K is given by the same expression (1.3.9) as in the noise-free case. This result is rather remarkable. It tells us that the feedback gain, calculated in the assumption of completely deterministic dynamics is, in fact, optimal in the stochastic case as well.

In the presence of nonvanishing noise and with the control turned on, the system will oscillate about the target state. The statistical measure of the amplitude of this oscillation is given by the state correlation matrix $\Phi = \langle \Delta\mathbf{x}_t \Delta\mathbf{x}_t^\dagger \rangle$, which can be easily found analytically, provided the process noise is not correlated with the system state, $\langle \Delta\mathbf{x}_t \mathbf{w}_t^\dagger \rangle = 0$. Indeed, the closed-loop system with feedback gain K is described by the dynamical equation

$$\Delta\mathbf{x}^{t+1} = (A - BK)\Delta\mathbf{x}^t + E\mathbf{w}^t. \tag{1.4.4}$$

Multiplying Eq. (1.4.4) by its transpose and taking the average yields

$$\Phi = (A - BK)\Phi(A - BK)^\dagger + E\Xi E^\dagger, \tag{1.4.5}$$

and since the matrix $A - BK$ is stable, the solution in the form of the convergent series is obtained:

$$\Phi = \sum_{n=0}^{\infty} (A - BK)^n E\Xi E^\dagger (A - BK)^{n\dagger}. \tag{1.4.6}$$

We note that Φ is a linear function of Ξ, so that the average deviation from the target state is linearly proportional to the strength of noise. As a result, the ratio of the two is an invariant quantity dependent only on the choice of feedback gain K. It is called the *noise amplification* factor and is defined thus:

$$\nu = \left[\frac{\langle |\Delta\mathbf{x}^t|^2 \rangle}{\langle |\mathbf{w}^t|^2 \rangle} \right]^{1/2} = \left[\frac{\mathrm{Tr}(\Phi)}{\mathrm{Tr}(\Xi)} \right]^{1/2}. \tag{1.4.7}$$

Clearly, the smaller ν is — the better the control setup can suppress noise. Examination of Eq. (1.4.2) with $Q = I$ and $R = 0$ shows that $V = \mathrm{Tr}(P_0 E\Xi E^\dagger) = \mathrm{Tr}(\Phi_0)$. As a result, the minimal value of the noise amplification factor

$$\nu = \left[\frac{\mathrm{Tr}(P_0 E\Xi E^\dagger)}{\mathrm{Tr}(\Xi)} \right]^{1/2} \tag{1.4.8}$$

is achieved for the optimal feedback gain $K = K_0$ calculated using Eqs. (1.3.8) and (1.3.9).

We repeat the numerical experiment of the previous section retaining the same values of system parameters and using the same feedback, but from now on applying uncorrelated random perturbations to each site of the lattice, which corresponds to

$$L_i(\mathbf{x}^t, \mathbf{w}^t, \mathbf{u}^t) = \delta_{i,1} u_1^t + \delta_{i,8} u_2^t + w_i^t, \tag{1.4.9}$$

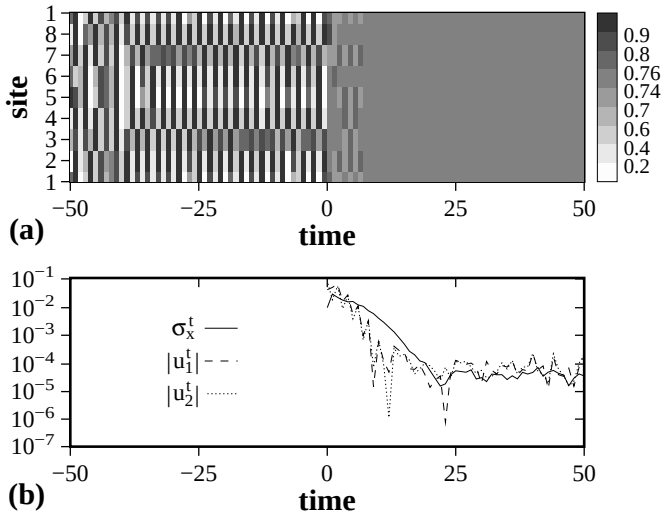

Abb. 1.4: State feedback control of the steady state S1T1 with noise: (a) system state, (b) its deviation σ_x^t from the target state and magnitude of control perturbations u_1^t and u_2^t. The amplitude of noise is $\sigma_w = 10^{-5}$. Feedback is turned on at $t = 0$.

and, consequently, $E = I$. Furthermore, we choose w_i^t as independent random variables uniformly distributed in the interval $[-\sigma_w, \sigma_w]$, so that $\Xi = (\sigma_w^2/3)I$. The state of the system before and after the control is turned on is presented in Fig. 1.4(a) for the noise amplitude $\sigma_w = 10^{-5}$. Large oscillations about the target state disappear after about ten iterations, as in the noise-free case, although after that, instead of converging to the uniform target state at a constant rate, the system settles into smaller amplitude oscillations driven by external noise, as evidenced by the standard deviation σ_x^t presented in Fig. 1.4(b) along with the magnitude of control perturbations.

When the noise cannot be considered small, minimizing the maximal strength of noise $\bar{\sigma}_w$ that the control scheme can tolerate becomes a much more important criterion than minimizing the noise amplification factor ν. In general, $\bar{\sigma}_w$ depends not only on ν, but also on the size of the basin of attraction $\mathcal{N}(\bar{\mathbf{x}})$ which, in turn, depends on the strength of feedback. For the CML (1.2.8), however, it was found numerically that setting $R = 0$ to obtain the smallest ν usually yields the largest $\bar{\sigma}_w$, thus satisfying both criteria.

We also found that the optimal control method outlined above is considerably more robust than the control methods based on the deterministic approach, such as the conventional multiparameter control algorithm proposed by Barreto and Grebogi [16]. For comparison we calculated the maximal amplitude of noise tolerated by each of the methods for the target state S1T1 of the lattice with $n_x = 8$ sites, $a = 4.0$ and $\epsilon = 0.33$. We obtained $\bar{\sigma}_w \approx 3 \times 10^{-3}$ for the former method versus $\bar{\sigma}_w \approx 10^{-7}$ for the latter, a difference of more than few orders of magnitude. Similar results were obtained for a number of other target states.

1.5 Control of Periodic Orbits

So far we only discussed the time-invariant control problem which is obtained when the target state is steady, i.e., has time period one. If the target state is periodic with period $\tau > 1$, the analysis does not change conceptually. However, a number of technical modifications of the algorithm have to be made in order to solve the problem using the formalism outlined in previous sections. Let us denote the target state $\bar{\mathbf{x}}^t$, where due to the periodicity $\bar{\mathbf{x}}^{t+\tau} = \bar{\mathbf{x}}^t$. Linearizing the evolution equation (1.2.8) about $\bar{\mathbf{x}}^t$ yields

$$\Delta\mathbf{x}^{t+1} = A^t\Delta\mathbf{x}^t + B^t\Delta\mathbf{u}^t + E^t\mathbf{w}^t, \tag{1.5.1}$$

where the Jacobian $A^t = MN^t$, the control matrix $B^t = \mathbf{D_u h}(\bar{\mathbf{x}}^t, \mathbf{0}, \mathbf{0})$, and the matrix $E^t = \mathbf{D_w h}(\bar{\mathbf{x}}^t, \mathbf{0}, \mathbf{0})$ all become time-varying and periodic in the index t. The stretching matrix N^t above is defined by generalizing (1.2.4):

$$N^t_{ij} = \partial_x f(\bar{x}^t_i, a)\delta_{i,j}. \tag{1.5.2}$$

Similarly to the noisy time-invariant case we find the optimal feedback by minimizing the functional (1.4.2) with the weights Q and R which can, in principle, be chosen time-periodic, thus acquiring the time index as well. The minimum is again reached for $\Delta\mathbf{u}^t = -K^t\Delta\mathbf{x}^t$, where the feedback gain now also becomes time-periodic:

$$K_t = (R_t + B_t^\dagger P_{t+1} B_t)^{-1} B_t^\dagger P_{t+1} A_t. \tag{1.5.3}$$

P^t denotes the time-periodic solution of the system of τ coupled Riccati equations

$$P_t = Q_t + A_t^\dagger P_{t+1} A_t - A_t^\dagger P_{t+1} B_t (R_t + B_t^\dagger P_{t+1} B_t)^{-1} B_t^\dagger P_{t+1} A_t, \tag{1.5.4}$$

which can be formally reduced to a single Riccati equation of larger dimensionality using the following ansatz.

Let us introduce the $\tau n_x \times \tau n_x$ cyclic-shift block matrix

$$Z = \begin{bmatrix} 0 & \cdots & 0 & I \\ I & \cdots & 0 & 0 \\ \vdots & \ddots & \vdots & \vdots \\ 0 & \cdots & I & 0 \end{bmatrix}, \tag{1.5.5}$$

consisting of $n_x \times n_x$ zero and unit blocks (we set $Z = I$ if $\tau = 1$), and form block-diagonal time-invariant matrices A, B, E, Q and R from the sequences of time-periodic matrices A^t, B^t, E^t, Q^t and R^t, respectively, according to the rule

$$A = \begin{bmatrix} A^1 & \cdots & 0 \\ \vdots & \ddots & \vdots \\ 0 & \cdots & A^\tau \end{bmatrix}. \tag{1.5.6}$$

Then the solution of the system of equations (1.5.4) is obtained by finding the block-diagonal solution

$$P = \begin{bmatrix} P^1 & \cdots & 0 \\ \vdots & \ddots & \vdots \\ 0 & \cdots & P^\tau \end{bmatrix}. \tag{1.5.7}$$

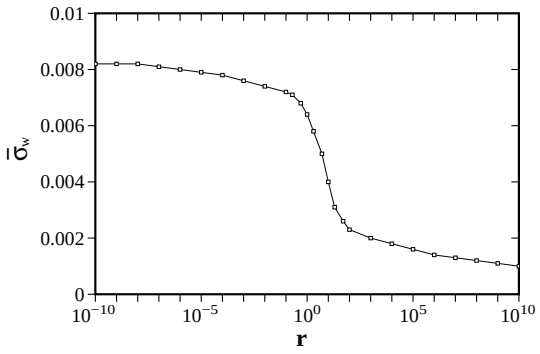

Abb. 1.5: Maximal noise amplitude tolerated by state feedback control: $\bar{\sigma}_w$ is plotted for the periodic state S8T4 as a function of r, where $R = rI$. Matrix $Q = I$ is kept constant.

of the Riccati equation

$$P = Q + A^\dagger Z^\dagger PZA - A^\dagger Z^\dagger PZB(R + B^\dagger Z^\dagger PZB)^{-1} B^\dagger Z^\dagger PZA. \tag{1.5.8}$$

Thus, from the control point of view, the time-periodic linear system (1.5.1) is effectively equivalent to the time-invariant linear system

$$\Delta \mathbf{X}^{t+1} = ZA\Delta \mathbf{X}^t + ZB\Delta \mathbf{U}^t + ZE\mathbf{W}^t. \tag{1.5.9}$$

The feedback gain (1.5.3) is by construction optimal for both deterministic and stochastic systems. The weight matrices can be further tuned according to the performance criterion selected in either case. For instance, in the stochastic case it usually more desirable to increase the tolerance of the control scheme to noise. Hence, for each target state we can set $Q = I$ and $R = rI$ and find the maximal noise strength $\bar{\sigma}_w$ for various r, thus determining the optimal weights.

Let us again take $a = 4.0$, $\epsilon = 0.33$ and $n_x = 8$. For these values of parameters the coupled map lattice defined by Eqs. (1.2.8) and (1.4.9) has a multitude of unstable periodic trajectories. We pick a period four nonuniform (S8T4) trajectory, which is invariant with respect to reflections about sites $i = 4$ and $i = 8$, as our target state. The control scheme obtained is rather robust and can withstand noise of considerable amplitude σ_w. As one can see from Fig. 1.5 the value of $\bar{\sigma}_w$ varies over almost an order of magnitude, reaching the maximum of approximately 8×10^{-3} for smallest r, i.e. $\bar{\sigma}_w$ is maximized by minimizing the noise amplification factor ν. Different target states, however, are sensitive to the choice of the relative magnitude of Q and R to a different degree, e.g., for the steady uniform target state $\bar{\sigma}_w \approx 3 \times 10^{-3}$ is essentially independent of the choice of weight matrices.

In order to achieve the best robustness properties we calculate the feedback gain (1.5.3) using $r = 0$. Since the target state S8T4 has period four, the feedback gain matrix obtained is also periodic with the same period. The state of the system, its deviation from the target state and the magnitude of applied control are presented in Fig. 1.6 for the largest amplitude of noise tolerated.

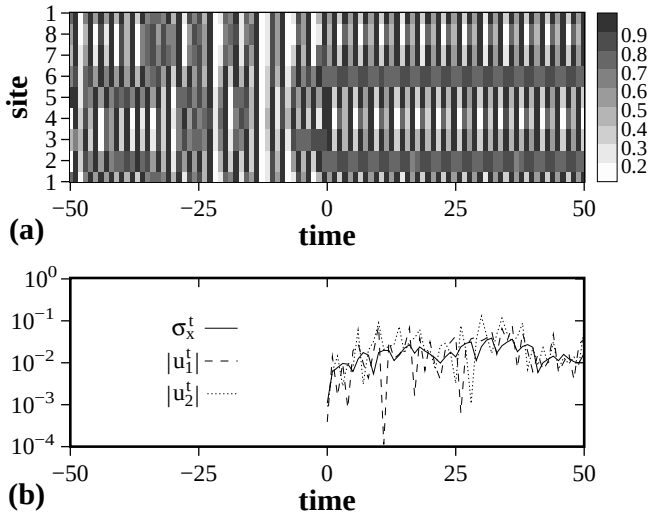

Abb. 1.6: State feedback control of the periodic state S8T4 with noise: (a) system state, (b) its deviation σ_x^t from the target state and magnitude of control perturbations u_1^t and u_2^t. The amplitude of noise is $\sigma_w = 8 \times 10^{-3}$. Feedback is turned on at $t = 0$.

1.6 State Reconstruction

If direct determination of the system state is inconvenient, impractical, or just impossible — the situation often encountered in real physical systems — a modification of the LQC method outlined in the previous sections can be used. In addition to the control structure that employs feedback we need to introduce another construction, usually called the *filter*, that would monitor, collect and process the available information about the system with the purpose of reconstructing its internal state with the best accuracy possible. Since the errors introduced by the filter become amplified by control, it is equally as important to have an optimal filter as it is to have optimal control. Optimal filtering techniques derived for the reconstruction problem [15] have much in common with the optimal control techniques. As a consequence, similar results often apply.

We are interested in reconstructing the system state only in the vicinity of the target state $\bar{\mathbf{x}}^t$, where the dynamics of the system is described with adequate precision by the linearized evolution equation (1.5.1). Assume that a single (or sometimes several) scalar output(s) $\mathbf{y}^t$ of the system can be measured. In general, the measurements are imperfect, with the deviation from the perfect values described by the measurement errors $\mathbf{v}^t$:

$$\mathbf{y}^t = \mathbf{G}(\mathbf{x}^t, \mathbf{v}^t). \tag{1.6.1}$$

For simplicity let us also assume that target state is time-invariant. Linearizing the output (1.6.1) in the vicinity of the target state and introducing the notation

$\Delta\mathbf{y}^t = \mathbf{G}(\mathbf{x}^t, \mathbf{v}^t) - \mathbf{G}(\bar{\mathbf{x}}, \mathbf{0})$ one obtains:

$$\Delta\mathbf{y}^t = C\Delta\mathbf{x}^t + D\mathbf{v}^t, \tag{1.6.2}$$

where $C = \mathbf{D}_\mathbf{x}\mathbf{G}(\bar{\mathbf{x}}, \mathbf{0})$ and $D = \mathbf{D}_\mathbf{v}\mathbf{G}(\bar{\mathbf{x}}, \mathbf{0})$.

In general, the problem of dynamical state reconstruction can be cast in a number of different ways. Here we pursue the one which is most easily treated in the framework of optimal control. Our goal is to use the available information about the system, i.e., the time series of control and output signals, to construct a vector $\Delta\hat{\mathbf{x}}^t$, which we call the *state estimate*, that would approximate the actual state $\Delta\mathbf{x}^t$. First of all, similarly to the dynamics of the actual state, the dynamics of the state estimate at time t should depend deterministically on the present value of the state estimate $\Delta\hat{\mathbf{x}}^t$, the control perturbation $\Delta\mathbf{u}^t$ and the output $\Delta\mathbf{y}^t$. Consistent with our linear approximation we obtain the general dynamical equation of the form

$$\Delta\hat{\mathbf{x}}^{t+1} = \hat{A}\Delta\hat{\mathbf{x}}^t + \hat{B}\Delta\mathbf{u}^t + \hat{K}\Delta\mathbf{y}^t, \tag{1.6.3}$$

where $\hat{A}$, $\hat{B}$ and $\hat{K}$ are some as yet undefined matrices. Next, notice that in the absence of noise and measurement errors, if the state estimate and the actual state coincide at time t_0, they should coincide at all later times $t > t_0$ as well, and, therefore, Eq. (1.6.3) should coincide with Eq. (1.2.2) upon substituting Eq. (1.6.2) with $\mathbf{v}^t = \mathbf{0}$ for arbitrary $\Delta\mathbf{u}^t$ and $\Delta\hat{\mathbf{x}}^t = \Delta\mathbf{x}^t$:

$$\Delta\mathbf{x}^{t+1} = (\hat{A} + \hat{K}C)\Delta\mathbf{x}^t + \hat{B}\Delta\mathbf{u}^t. \tag{1.6.4}$$

This requires $\hat{A} = A - \hat{K}C$ and $\hat{B} = B$, so that Eq. (1.6.3) yields the dynamical equation

$$\Delta\hat{\mathbf{x}}^{t+1} = A\Delta\hat{\mathbf{x}}^t + B\Delta\mathbf{u}^t + \hat{K}(\Delta\mathbf{y}^t - C\Delta\hat{\mathbf{x}}^t), \tag{1.6.5}$$

where $\hat{K}$ is called the *filter gain* matrix. Finally, we need $\Delta\hat{\mathbf{x}}^t$ to be a good estimate of the actual state, i.e., the difference $\Delta\tilde{\mathbf{x}}^t = \Delta\mathbf{x}^t - \Delta\hat{\mathbf{x}}^t$ between the actual state and its estimate should be small even when finite noise or measurement errors are present. Subtracting Eq. (1.6.5) from Eq. (1.4.1) and substituting Eq. (1.6.2) we obtain

$$\Delta\tilde{\mathbf{x}}^{t+1} = (A - \hat{K}C)\Delta\tilde{\mathbf{x}}^t + \tilde{\mathbf{w}}^t, \tag{1.6.6}$$

where $\tilde{\mathbf{w}}^t = E\mathbf{w}^t - \hat{K}D\mathbf{v}^t$ denotes the sum of all stochastic terms in Eq. (1.6.6). Assuming the measurement errors are random, unbiased, δ-correlated in time,

$$\langle \mathbf{v}_t \mathbf{v}_{t'}^\dagger \rangle = \Theta\, \delta_{tt'}, \tag{1.6.7}$$

and uncorrelated with the process noise, $\langle \mathbf{w}_t \mathbf{v}_{t'}^\dagger \rangle = 0$, we conclude that $\tilde{\mathbf{w}}^t$ is a stationary zero-mean random process with correlation

$$\langle \tilde{\mathbf{w}}_t \tilde{\mathbf{w}}_{t'}^\dagger \rangle = (\hat{K}\hat{R}\hat{K}^\dagger + \hat{Q})\, \delta_{tt'}, \tag{1.6.8}$$

where we introduced the shorthand notations $\hat{R} = D\Theta D^\dagger$ and $\hat{Q} = E\Xi E^\dagger$.

Observe that Eq. (1.6.6) has the same form as Eq. (1.4.4) for the closed-loop system. It turns out [15] that, if the assumptions made above hold, the stochastic

time-invariant optimal state reconstruction problem defined by Eqs. (1.6.2), (1.6.5) is formally equivalent to the deterministic time-invariant optimal control problem defined by Eq. (1.2.2), with the following correspondence between parameters: $A \leftrightarrow A^\dagger$, $B \leftrightarrow C^\dagger$, $Q \leftrightarrow \hat{Q}$, $R \leftrightarrow \hat{R}$, $P \leftrightarrow S$ and $K \leftrightarrow \hat{K}^\dagger$.

In order to guarantee the existence of a positive definite solution S to the respective Riccati equation the pair of matrices $(A^\dagger, C^\dagger)$ should be controllable. This condition is equivalent to the dual condition of *observability* for the matrix pair (A, C) and ensures that the state of the system can be reconstructed given the measurement of the output. More formally, the dynamical system defined by Eqs. (1.2.2) and (1.6.2), or the pair (A, C), is said to be observable if for any times $t_f - t_i \geq n_x$ the initial state $\Delta\mathbf{x}^{t_i} = \Delta\mathbf{x}_i$ can be determined from the measurement of control perturbation $\Delta\mathbf{u}^t$ and output $\Delta\mathbf{y}^t$ in the interval $t \in [t_i, t_f]$.

The generalization to periodic target states is rather trivial and can be accomplished using the procedure discussed in the previous section. Assuming the period of the target state is $\tau \geq 1$, we construct the constant matrices A, B, C, Q, R, $\hat{Q}$ and $\hat{R}$ from the respective time-periodic matrices according to the rule (1.5.6). Putting all the pieces together, one finally concludes that the time-periodic output feedback control problem with additive noise

$$\begin{aligned} \Delta\mathbf{x}^{t+1} &= A^t\Delta\mathbf{x}^t + B^t\Delta\mathbf{u}^t + E^t\mathbf{w}^t, \\ \Delta\mathbf{y}^t &= C^t\Delta\mathbf{x}^t + D^t\mathbf{v}^t, \end{aligned} \tag{1.6.9}$$

requires the feedback $\Delta\mathbf{u}^t$, calculated according to the equations

$$\begin{aligned} \Delta\hat{\mathbf{x}}^{t+1} &= A^t\Delta\hat{\mathbf{x}}^t + B^t\Delta\mathbf{u}^t + \hat{K}^t(\Delta\mathbf{y}^t - C^t\Delta\hat{\mathbf{x}}^t), \\ \Delta\mathbf{u}^t &= K^t\Delta\hat{\mathbf{x}}^t. \end{aligned} \tag{1.6.10}$$

The optimal feedback gain K^t is found using equations (1.5.3) and (1.5.8), while the optimal filter gain $\hat{K}^t$ is determined by

$$\hat{K}_t = A_t S_{t-1} C_t^\dagger (\hat{R}_t + C_t S_{t-1} C_t^\dagger)^{-1}, \tag{1.6.11}$$

where S^1 through S^τ are the blocks found on the diagonal of the block-diagonal solution S of the Riccati equation

$$S = \hat{Q} + AZSZ^\dagger A^\dagger - AZSZ^\dagger C^\dagger (\hat{R} + CZSZ^\dagger C^\dagger)^{-1} CZSZ^\dagger A^\dagger. \tag{1.6.12}$$

In spatially extended systems it is usually much more convenient to extract information about the system locally at a number of distinct spatial locations. Indeed, most sensors provide information of extremely local character. For the coupled map lattice (1.2.8) this implies that the state of each sensor depends only on the state of the lattice in some small neighborhood of that sensor. Similarly to the number of control parameters n_u, the number of scalar output signals n_y is bounded from below for highly symmetric target states by the observability condition, which is a natural consequence of the above mentioned duality. Placing sensors at the pinnings and assuming that the neighborhood only includes the pinning site itself, we conclude that $C = B^\dagger$, so that the observability condition is satisfied automatically and $n_y = n_u$.

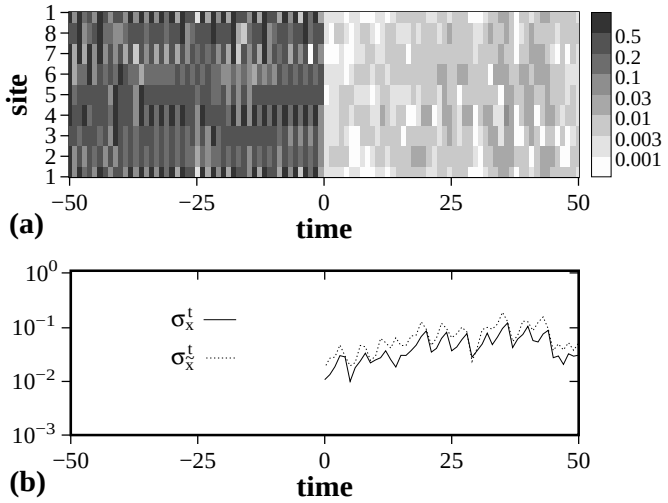

Abb. 1.7: Output feedback control of the periodic state S8T4 with noise and imperfect measurements: (a) difference $\Delta\tilde{\mathbf{x}}^t$ between the actual and the estimated system state, (b) deviation σ_x^t from the target state and the reconstruction error $\sigma_{\tilde{x}}^t$. The amplitudes of the process noise and measurement errors are $\sigma_w = 10^{-3}$ and $\sigma_v = 10^{-5}$. Feedback and filtering are turned on simultaneously at $t = 0$.

In the case of output feedback control one cannot measure the distance to the target trajectory directly because the actual state of the system is not available. However, if the system is sufficiently close to the point $\bar{\mathbf{x}}^{t_0}$ at time t, the difference $\mathbf{y}^t - G(\bar{\mathbf{x}}^{t_0}, \mathbf{0})$ should be small. Verifying this condition at a succession of times usually ensures that the system indeed closely follows the trajectory $\bar{\mathbf{x}}^{t_0}, \bar{\mathbf{x}}^{t_0+1}, \cdots$. The state estimate $\Delta\hat{\mathbf{x}}^t$ can be reset to zero when the system is far from the target state. Filtering is turned on simultaneously with feedback when the system approaches one of the points $\bar{\mathbf{x}}^{t_0}$, $t_0 = 1, \cdots, \tau$ of the target trajectory. We illustrate this algorithm using the same target state, system parameters and location of pinnings as in the previous section. The difference $\Delta\tilde{\mathbf{x}}^t$ between the actual and the estimated state of the system is plotted in Fig. 1.7(a), and Fig. 1.7(b) shows the deviation σ_x^t from the target trajectory and the reconstruction error

$$\sigma_{\tilde{x}}^t = \left[\frac{1}{n_x} \sum_{i=1}^{n_x} |\Delta\tilde{x}_i^t|^2 \right]^{1/2} . \tag{1.6.13}$$

1.7 Density of Pinnings

1.7.1 Lattice Partitioning

To facilitate practical implementation the control algorithm presented above should be easily extendable to systems of arbitrary size. However, even though it is the-

oretically possible to control the deterministic coupled map lattice of any length using just two pinning sites, practical limitations require the introduction of additional pinning sites as the length of the lattice grows. Since the total number of pinnings changes, when the lattice becomes large, it makes more sense to talk about the minimal density of pinnings, or the maximal number of lattice sites per pinning, that allows successful control under given conditions.

Furthermore, since coupling between lattice sites is local, the feedback u_m^t only affects the dynamics of the sites i which are sufficiently close to the pinning site i_m. Conversely, we expect the feedback u_m^t to be essentially independent of the state of the lattice sites i far away from the pinning i_m. Using this observation allows one to simplify the construction of the control scheme substantially by explicitly defining the neighborhood of each pinning i_m that contributes to and is affected by the feedback u_m^t. We thus naturally arrive at the idea of distributed control.

By arranging the pinnings regularly we ensure that the lattice is partitioned into a number of identical subdomains described by identical evolution equations. To simplify the analysis we assume that each subdomain contains the minimal number of pinning sites, i.e., two. Placing the pinnings at the boundaries of subdomains allows one to choose boundary conditions for each of the subdomains at will, so we assume that boundary conditions are periodic. This effectively decouples adjacent subdomains, which can now be treated independently. The general problem of controlling the lattice of arbitrary length n_x is thus reduced to the simpler problem of controlling the lattice of length $n_d \ll n_x$ with two pinning sites, which was studied in detail in the preceding sections.

Indeed, let the domain span the sites i_1 through $i_2 = i_1 + n_d - 1$ of the lattice. Then arbitrary boundary conditions

$$\begin{aligned} x_{i_1-1}^t &= \psi_1(x_{i_1}^t, \cdots, x_{i_2}^t), \\ x_{i_2+1}^t &= \psi_2(x_{i_1}^t, \cdots, x_{i_2}^t) \end{aligned} \tag{1.7.1}$$

can be imposed by adjusting the feedback as follows

$$\begin{aligned} \Delta u_1^t &\rightarrow \Delta u_1^t + \epsilon f(\psi_1(x_{i_1}^t, \cdots, x_{i_2}^t)) - \epsilon f(x_{i_1-1}^t), \\ \Delta u_2^t &\rightarrow \Delta u_2^t + \epsilon f(\psi_2(x_{i_1}^t, \cdots, x_{i_2}^t)) - \epsilon f(x_{i_2+1}^t), \end{aligned} \tag{1.7.2}$$

which only requires the knowledge about the state of the system inside the subdomain and at two adjacent sites $i_1 - 1$ and $i_2 + 1$. If the exact form of the evolution equation (1.2.8) is not known, the linearization of Eqs. (1.7.2) can be used instead. The nonlinear version, however, has a significant additional benefit associated with it: nonlinear decoupling of adjacent subdomains dramatically decreases the capture time by decreasing the effective dimensionality of the system.

We demonstrate the effectiveness of nonlinear decoupling by stabilizing the target state S1T1 of the CML defined by equations (1.2.8), (1.2.11) with $a = 4.0$ and $\epsilon = 0.33$. The lattice with $n_x = 128$ sites was divided into subdomains of length $n_d = 8$, each controlled by two pinning sites placed at the boundaries. The results presented in Fig. 1.8 show the evolution of the system from the initial condition chosen to be a collection of random numbers in the interval $[0, 1]$. The average time to achieve control in each of the subdomains, t_c, is seen to be of order 10^5

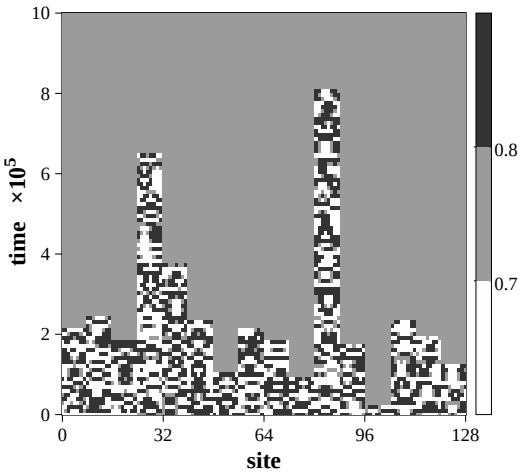

Abb. 1.8: Stabilizing steady uniform state: a large lattice ($n_x = 128$) is controlled by an array of double pinning sites, placed at the boundaries of subdomains with length $n_d = 8$. The state of the system was plotted at each 10^4th step.

iterations even though the subdomains were chosen relatively small. In general, t_c grows exponentially with the pointwise dimension of the attractor, $t_c \propto (\delta x)^{-\mathcal{D}}$, and since $\mathcal{D} \propto n_d$ for large n_d, the time t_c can become prohibitively large, imposing restrictions on the largest size of the subdomain.

1.7.2 State Feedback

The major factor limiting our ability to locally control arbitrarily large systems with local interactions, however, is noise. The strength of noise and the values of system parameters determine the maximal length $\bar{n}_x$ of the lattice that can be controlled with two pinnings placed at the boundaries, which subsequently defines the minimal density of pinning sites $\rho = 2/\bar{n}_x$. It is interesting to note that, at least for the target state S1T1, the length $\bar{n}_x$ can be estimated analytically [21] with a rather good precision using the conditions of controllability and observability, highlighting their fundamental role in the control problem.

First, assume that the state of the system can be determined directly at any time, so that state feedback control can be used. In the deterministic case the controllability condition determines whether there exists a control sequence $\Delta\mathbf{u}^{t_i}, \cdots, \Delta\mathbf{u}^{t_i+n_x-1}$, bringing an arbitrary initial state $\Delta\mathbf{x}^{t_i}$ to an arbitrary final state $\Delta\mathbf{x}^{t_f}$, where $t_f = t_i + n_x$. In the presence of noise and without assuming any functional relationship between the state and the feedback we can write

$$\Delta\mathbf{x}^{t_i+n_x} = (A)^{n_x}\Delta\mathbf{x}^{t_i} + \sum_{k=1}^{n_x}(A)^{n_x-k}B\Delta\mathbf{u}^{t_i+k-1} + \sum_{k=1}^{n_x}(A)^{n_x-k}E\mathbf{w}^{t_i+k-1}. \quad (1.7.3)$$

This equation is not exact, it is only an approximation of the exact nonlinear

evolution equation (1.2.8), valid when both $\Delta\mathbf{x}^t$ and $\Delta\mathbf{u}^t$ are sufficiently small for all times $t = t_i, \cdots, t_f - 1$, as discussed in section 1.3. The linearization (1.4.1) on which Eq. (1.7.3) is based is valid for arbitrary $\Delta\mathbf{u}^t$. However, since feedback directly perturbes the state of the system its magnitude is limited by nonlinearities to the same range δx as the local deviation Δx_i^t from the target state. Therefore, the control sequence should satisfy both Eq. (1.7.3) and the restriction

$$|\Delta u_m^t| < \delta x, \quad m = 1, 2, \quad t = t_i, \cdots, t_f - 1. \tag{1.7.4}$$

Taking $\Delta\mathbf{x}^{t_i} = \Delta\mathbf{x}^{t_f} = \mathbf{0}$ (the initial and final states coincide with the target state) Eq. (1.7.3) can be rewritten as

$$\mathbf{z} = -\sum_{k=1}^{n_x} (A)^{n_x-k} E\mathbf{w}^{t_i+k-1} = \mathbf{0} + \sum_{k=1}^{n_x}\sum_{m=1}^{n_u} (A)^{n_x-k}\mathbf{b}_m\, \Delta u_m^{t_i+k-1}, \tag{1.7.5}$$

which is formally equivalent to the problem of finding the feedback sequence bringing the system from the initial state $\Delta\mathbf{x}_i = \mathbf{0}$ to the final state $\Delta\mathbf{x}_f = \mathbf{z}$ in n_x steps in the absence of noise.

Again we assume that the process noise $\mathbf{w}^t$ is represented by a vector whose components w_i^t are independent random variables uniformly distributed in the interval $[-\sigma_w, \sigma_w]$. Noise is amplified roughly by a factor of γ per iteration, where γ is the largest eigenvalue (1.2.15) of the Jacobian. As a consequence, the left hand side of Eq. (1.7.5) can also be represented as a vector with random components z_i distributed in the interval $[-\beta\sigma_w, \beta\sigma_w]$, where

$$\beta = \sum_{t=0}^{n_x-1} |\gamma|^t \approx \frac{|\gamma|^{n_x}}{|\gamma| - 1}. \tag{1.7.6}$$

It could be argued that for the control to suppress any sequence of random perturbations $\mathbf{w}^t$, every term $(A)^{n_x-k}\mathbf{b}_m\, \Delta u_m^{t_i+k-1}$ on the right hand side of Eq. (1.7.5) should be of the same order of magnitude as the amplified noise $\mathbf{z}$. The vector $\mathbf{b}_m\, \Delta u_m^{t_i+k-1}$ represents local perturbation $\delta x_{i_m}^t = u_m^{t_i+k-1}$ introduced at the site i_m at time $t = t_i + k - 1$, while the matrix $(A)^{n_x-k}$ describes the propagation of that perturbation throughout the lattice. According to the structure of the matrix A local perturbation at site i_m affects the dynamics of the remote site j only after propagating a distance $l = |i_m - j|$ in time $\Delta t = l$, decaying (or being amplified) by a factor of $\alpha\epsilon$ per iteration. Consequently, the state of site j at time t_f will be affected by control Δu_m^t applied only at times $t_i, \cdots, t_i + n_x - l - 1$. The perturbation applied at $t = t_i + n_x - l - 1$ is amplified the least and yields the order of magnitude relation

$$\delta x = O\left((\alpha\epsilon)^{-l}\beta\sigma_w\right). \tag{1.7.7}$$

Due to the periodic boundary condition, $0 \le l \le n_x/2$. On the other hand, δx can be estimated by equating the magnitude of the linear term with the magnitude of the next nonlinear term in the Taylor expansion of the local map function:

$$f(\bar{x} + \delta x, a) = f(\bar{x}, a) + \kappa(\delta x + \mu(\delta x)^2 + \cdots). \tag{1.7.8}$$

For instance, the logistic map (1.2.11) gives $\delta x \sim \mu^{-1} = 2\bar{x} - 1 = 1 - 2a^{-1}$. As a result, we obtain the following estimate on the size of the controllable domain for an arbitrary coupled map lattice with the quadratic nonlinearity:

$$\bar{n}_x^{(1)}(\sigma_w) = -\frac{\ln(\mu\sigma_w) + \ln(\xi)}{\ln(\zeta)}, \tag{1.7.9}$$

which is rather similar to the one obtained by Aranson *et al.* [23] for the lattice with asymmetric coupling. Parameters ξ and ζ in Eq. (1.7.9) are defined by Eq. (1.7.7) with l giving the tightest bound. For $0 < \epsilon < 0.5$ (and $l = n_x/2$) we get

$$\xi = [|\alpha| - 1]^{-1}, \qquad \zeta = |\alpha|^{1/2}\epsilon^{-1/2}, \tag{1.7.10}$$

while for $0.5 \leq \epsilon < 1$ (and $l = 0$) we obtain

$$\xi = [|\alpha|(4\epsilon - 1) - 1]^{-1}, \qquad \zeta = |\alpha|(4\epsilon - 1). \tag{1.7.11}$$

We should note that the estimate derived in [21] is only valid in the assumption of strong local instability, $|\alpha| \gg 1$, and is obtained as the limit of Eq. (1.7.9) with $\mu = 1$ and $\xi = 1$.

Another method for the calculation of $\bar{n}_x(\sigma_w)$ was proposed by Socolar and Egolf [24], who suggested to use the actual feedback gain matrix K to obtain more precise results for a specific control scheme. As we have seen in section 1.4, when the linear equation is perturbed by the noise of amplitude σ_w, one can estimate the average deviation from the target trajectory as $\sigma_x = \nu\sigma_w$, where ν is the noise amplification factor defined by Eq. (1.4.7). In a nonlinear system we instead have

$$\sigma_x = \nu(\sigma_w^2 + \sigma_{xx}^2)^{1/2}, \tag{1.7.12}$$

where σ_{xx} is the error resulting from ignoring the effect of nonlinear terms in Eq. (1.4.1). For a coupled map lattice with the quadratic nonlinearity one obtains $\sigma_{xx} = \mu\sigma_x^2$ and thus

$$\sigma_x^2 = \nu^2(\sigma_w^2 + \mu^2\sigma_x^4). \tag{1.7.13}$$

This is a quadratic equation in σ_x^2 which has solutions only when

$$\nu \leq \bar{\nu}(\sigma_w) = (2\mu\sigma_w)^{-1/2}, \tag{1.7.14}$$

thus determining the critical noise amplification factor. For $\nu > \bar{\nu}(\sigma_w)$ the effect of nonlinear terms can no longer be ignored and the control scheme breaks down. In principle, one can stop here and numerically evaluate the length of the system at which $\nu = \bar{\nu}(\sigma_w)$, thus obtaining the required functional dependence $\bar{n}_x(\sigma_w) = n_x(\bar{\nu}(\sigma_w))$ for a specific K.

However, making one more step allows one to easily extract the analytic dependence on the strength of noise. It can be argued that for any K the noise amplification factor depends exponentially on the length of the system

$$\nu = \chi\eta^{n_x}, \tag{1.7.15}$$

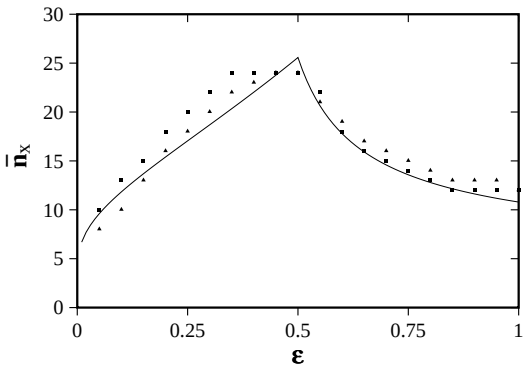

Abb. 1.9: The largest length of the lattice which can be stabilized with two pinning sites using state feedback control: theoretical estimates $\bar{n}_x^{(1)}$ (solid line) and $\bar{n}_x^{(2)}$ (triangles), and numerical results (squares) obtained with the process noise of amplitude $\sigma_w = 10^{-8}$ as functions of coupling ϵ for $a = 4.0$.

where both χ and η are functions of the system parameters α and ϵ and the feedback gain matrix K. Plugging Eq. (1.7.14) into (1.7.15) yields the final result in the form similar to Eq. (1.7.9):

$$\bar{n}_x^{(2)}(\sigma_w) = -\frac{\ln(\mu\sigma_w) + \ln(2\chi^2)}{\ln(\eta^2)}. \tag{1.7.16}$$

Two important conclusion can be drawn from this result. First of all, even though the length $\bar{n}_x$ does depend on a particular choice of the feedback gain, this dependence is rather weak, because it is attenuated by the logarithmic function, so that the obtained estimate is valid for any typical feedback gain that stabilizes the system. Second, the dependence on the strength of noise is also logarithmic and weak, however, the magnitude of σ_w is that crucial parameter that ultimately determines the scale for both $\bar{n}_x$ and the minimal density of pinning sites ρ.

The maximal length of the system, that can actually be stabilized by the LQC method with two pinning sites placed next to each other, is obtained numerically by choosing the target state as the initial condition and monitoring the evolution of the closed-loop system in the presence of process noise $\mathbf{w}^t$ of amplitude σ_w, applying feedback calculated using the formula (1.3.9) with $Q = I$ and $R = 0$. As seen from Fig. 1.9, this length is quite large for a moderate level of noise and is rather close to the values where the controllability breaks down according to Eq. (1.7.9). The agreement between the numerical results and theoretical estimates (1.7.9) and (1.7.16) is not perfect, although it is surprisingly good taking into account the order of magnitude arguments used in the derivations. The choice of the noise level was motivated by the need to separate the effect of the deviations σ_{xx} introduced by nonlinearity from the precision of numerical calculations $\sigma_n = O(10^{-16})$ in the evaluation of the feedback gain. Since $\sigma_w/\sigma_{xx} = O(1)$, one needs $1 \gg \sigma_w \gg \sigma_n$, so $\sigma_w = 10^{-8}$ was taken here (as opposed to $\sigma_w = 10^{-14}$ used in [21]).

The minimal density of pinning sites is reduced substantially by replacing equally spaced single pinnings with equally spaced paired pinnings. For the uniform steady target state S1T1, $a = 4.0$ and $\epsilon = 0.4$, for example, the estimate (1.7.9) gives $\rho_2 = 2/n_d = 1/11$ for the noise level $\sigma_w = 10^{-8}$ (the actual value of $1/12$ is even lower as seen from Fig. 1.9). If single pinnings are used instead, Eq. (1.2.17) demands $\rho_1 = 1/n_d = 1/2 \gg \rho_2$ even in the absence of noise.

1.7.3 Output Feedback

Finally, consider the output feedback control of the target state S1T1. Let us assume that the state of the system cannot be determined directly. Instead it has to be reconstructed using the measurements at the pinnings, i.e., using the time series of the lattice variables $x^t_{i_1}$ and $x^t_{i_2}$. As we noted in section 1.6, this setup dictates that $C = B^\dagger$ in Eq. (1.6.9). To avoid unnecessarily complicating the problem we also assume that the measurements are perfect, $\mathbf{v}^t = \mathbf{0}$.

In order to estimate $\bar{n}_x$ with these assumptions we will need to exploit both the controllability and the observability conditions. First, the state of the system has to be reconstructed using n_x consecutive measurements of the variables at the pinning sites. However, because of the nonzero process noise the reconstructed state will deviate from the actual state. Arguments similar to the ones used in deriving Eq. (1.7.7) allow one to estimate the order of magnitude of the reconstruction error at a lattice site with distance l to the closest pinning:

$$\delta\tilde{x}_l = O\left((\alpha\epsilon)^{-l}\beta\sigma_w\right). \tag{1.7.17}$$

Since the reconstruction error $\delta\tilde{x}_l$ is substantially larger than the strength of noise σ_w, the former has to be substituted for the latter in Eq. (1.7.7) yielding

$$\delta x = O\left((\alpha\epsilon)^{-2l}\beta^2\sigma_w\right). \tag{1.7.18}$$

Eventually, we obtain the following estimate of the maximal size:

$$\bar{n}_x^{(3)}(\sigma_w) = -\frac{\ln(\mu\sigma_w) + \ln(\xi^2)}{2\ln(\zeta)} \approx \frac{\bar{n}_x^{(1)}(\sigma_w)}{2}, \tag{1.7.19}$$

i.e., one half of the size of the lattice that can be stabilized using state feedback. This result can be understood intuitively: when output feedback is used, a signal in the system has to travel twice the distance in twice the time, first from a remote lattice site to the pinnings, carrying information about the state of the system, and then back in the form of feedback. This is effectively equivalent to doubling the size of the lattice, hence the factor of one half.

The same result can be obtained using the noise amplification factor. Observing that according to our assumptions $A^\dagger = A$, $\hat{R} = 0$ and $\hat{Q} = (\sigma^2/3)EE^\dagger$, we conclude that the filter gain and the feedback gain calculated for $R = 0$ and $Q = qEE^\dagger$, are directly related[2], $\hat{K} = K^\dagger$, as are the solutions of the Riccati equations,

[2] This is a general result: as long as $A = A^\dagger$ and $C = B^\dagger$, taking $\hat{K} = K^\dagger$ guarantees that the filter is stable even if the feedback gain K is not optimal.

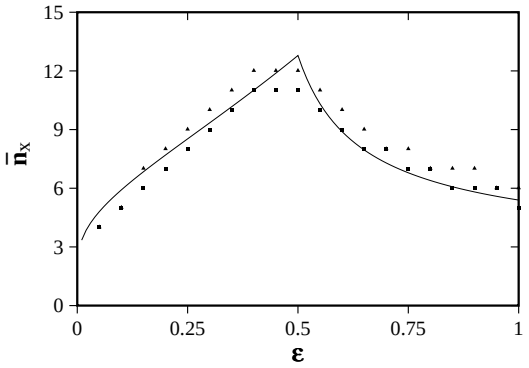

Abb. 1.10: The largest length of the lattice which can be stabilized with two pinning sites using output feedback control: theoretical estimates $\bar{n}_x^{(3)}$ (solid line) and $\bar{n}_x^{(4)}$ (triangles) and numerical results (squares) obtained with the process noise of amplitude $\sigma_w = 10^{-8}$ as functions of coupling ϵ for $a = 4.0$. The measurement errors were assumed to be negligible.

$S = P$. Therefore, the evolution equation (1.6.6) for the reconstruction error reduces to

$$\Delta\tilde{\mathbf{x}}^{t+1} = (A - BK)^\dagger \Delta\tilde{\mathbf{x}}^t + E\mathbf{w}^t. \tag{1.7.20}$$

Comparing Eq. (1.7.20) with the closed-loop evolution equation (1.2.6) for the state $\Delta\mathbf{x}^t$, we conclude that the respective noise amplification factors are equal, $\nu = \tilde{\nu}$.

Since both the process noise and the deviation caused by nonlinear terms are amplified first by the filter and then by the feedback, Eq. (1.7.12) has to be modified to read

$$\sigma_x = \tilde{\nu}\nu(\sigma_w^2 + \sigma_{xx}^2)^{1/2}, \tag{1.7.21}$$

with the subsequent change in the condition determining when the linear control breaks down:

$$\bar{\nu}(\sigma_w) = (2\mu\sigma_w)^{-1/4}. \tag{1.7.22}$$

Plugging this result into Eq. (1.7.15) yields

$$\bar{n}_x^{(4)}(\sigma_w) = -\frac{\ln(\mu\sigma_w) + \ln(2\chi^4)}{2\ln(\eta^2)} \approx \frac{\bar{n}_x^{(3)}(\sigma_w)}{2}. \tag{1.7.23}$$

We compare the theoretical predictions (1.7.19) and (1.7.23) with the actual numerical results for the CML subjected to the noise of amplitude $\sigma_w = 10^{-8}$ in Fig. 1.10. The target state S1T1 is stabilized using output feedback control (1.6.10), where the feedback gain K is calculated using Eq. (1.3.9) with $Q = I$ and $R = 0$ and the filter gain is set to $\hat{K} = K^\dagger$. Once again we conclude that the numerical results are in very good agreement with the theoretical estimates based on the assumption that the breakdown of linear control is caused by the interplay between the stochasticity and the nonlinearity of the evolution equation (1.2.8).

1.8 Summary

Reviewing the obtained results one can conclude that the general problem of optimal control of spatially extended chaotic dynamical systems with noise can be split into two major parts. The first part consists of analyzing how the spatial structure of the system affects the control algorithm and use the results of this analysis to determine the spatial structure of the control plant that is both effective and practically realizable. The second part consists of finding the optimal control perturbation driving the system towards the target state based on the available information about the state of the system.

By considering the simplified model that nevertheless preserves the defining features of a general spatially extended dynamical system such as symmetry and locality we hope to determine the basic ingredients of a control algorithm that should be applicable to a typical system of this class. Below we attempt to summarize these ingredients in most general terms.

The first major ingredient is the local nature of the control algorithm. Even though in certain cases global control might be used quite successfully, in general, the locality significantly simplifies the analysis of both the interaction between the system and the control plant, and the structure of the control plant itself. Besides, the locality makes the control algorithm easily scalable and facilitates practical implementation of the control strategy.

The second major ingredient is the proper mutual arrangement of the localized regions where the dynamics of the system is perturbed by the control plant. Choosing this arrangement in accordance with the underlying symmetries of the system affords a significant reduction of the complexity with simultaneous increase in the flexibility of the control algorithm, allowing it to control target states with arbitrary spatiotemporal properties, requiring a smaller density of such localized regions per unit length of the system. One particular arrangement deserves special attention. We determined that, if the noise level is sufficiently small, a system with translational (rotational) invariance and parity symmetry can be controlled by dynamically adjusting the boundary conditions. This can be considered as a "nonintrusive" control that requires minimal modification of the controlled system and can be implemented rather easily in a variety of applications.

The third and final ingredient of a general control algorithm is the stochastic optimal control method. The numerical results obtained indicate that the control methods based on the deterministic approach are considerably less robust, i.e., have much smaller basins of attraction and can tolerate only a small fraction of noise easily suppressed by the stochastic optimal control, especially in the weak coupling limit. Additionally, by subdividing the system into a number of noninteracting subsystems, the combination of the optimal control and filtering techniques with the local structure of the control plant yields a dramatic decrease in the average time required to capture the trajectory of the system, exploring its chaotic attractor, by linear control.

Bibliography

[1] C. Lee, J. Kim, D. Bobcock and R. Goodman, Phys. Fluids, **9**, 1740 (1997).

[2] A. Pentek, J. B. Kadtke, and Z. Toroczkai, Phys. Lett. A **224**, 85 (1996).

[3] V. Petrov, M. F. Crowley, K. Showalter, Physica D **84**, 12 (1995).

[4] A. Garfinkel, M. L. Spano, W. L. Ditto, and J. N. Weiss, Science, **257**, 1230 (1992).

[5] S. J. Schiff, K. Jerger, D. H. Duong, T. Chang, M. L. Spano, and W. L. Ditto, Nature, **370**, 615 (1994).

[6] V. Petrov, M. J. Crowley, and K. Showalter, Phys. Rev. Lett. **72**, 2955 (1994).

[7] P. Colet, R. Roy, and K. Weisenfeld, Phys. Rev. E **50**, 3453 (1994); M. E. Bleich, D. Hochheiser, J. V. Moloney, and J. E. S. Socolar, Phys. Rev. E **55**, 2119 (1997).

[8] C. Lourenco and A. Babloyantz, Int. J. Neu. Sys, **7**, 507 (1996).

[9] H. Gang and Q. Zhilin, Phys. Rev. Lett. **72**, 68 (1994).

[10] H. Gang and H. Kaifen, Phys. Rev. Lett. **71**, 3794 (1993); V. Petrov, E. Mihaliuk, S. K. Scott, and K. Showalter, Phys. Rev. E **51**, 3988 (1995);

[11] M. Ding, W. Yang, V. In, W. L. Ditto, M. L. Spano, and B. Gluckman, Phys. Rev. E **53**, 4334 (1996).

[12] J. Warncke, M. Bauer and W. Martienssen, Europhys. Lett. **25**, 323 (1994).

[13] M. A. Rhode, J. Thomas and R. W. Rollins, Phys. Rev. E **54**, 4880 (1996).

[14] R. O. Grigoriev and M. C. Cross, Phys. Rev. E **57**, 1550 (1998).

[15] R. F. Stengel, *Stochastic Optimal Control: Theory and Application* (J. Wiley, New York, 1986).

[16] E. Barreto and C. Grebogi, Phys. Rev. E **52**, 3553 (1995).

[17] E. Ott, C. Grebogi and J. A. Yorke, Phys. Rev. Lett. **64**, 1196 (1990).

[18] K. Kaneko, Prog. Theor. Phys. **72**, 480 (1984).

[19] D. Auerbach, Phys. Rev. Lett. **72**, 1184 (1994).

[20] Y. S. Kwon, S. W. Ham, and K. K. Lee, Phys. Rev. E **55**, 2009 (1997).

[21] R. O. Grigoriev, M. C. Cross, and H. G. Schuster, Phys. Rev. Lett. **79**, 2795 (1997).

[22] J. F. Lindner and W. L. Ditto, Appl. Mech. Rev. **48**, 795 (1995).

[23] I. Aranson, D. Golomb and H. Sompolinsky, Phys. Rev. Lett. **68**, 3495 (1992).

[24] J. E. S. Socolar, D. Egolf, to appear in Phys. Rev. E **57**(5) (1998).